CHIN. PHYS. LETT. Vol. 36, No. 6 (2019) 063201

Carrier Envelope Phase Description for an Isolated Attosecond Pulse by Momentum Vortices *

Meng Li(李猛)[1,2], Gui-zhong Zhang(张贵忠)[1**], Xin Ding(丁欣)[1], Jian-quan Yao(姚键铨)[1]

[1] *College of Precision Instrument and Optoelectronics Engineering, Tianjin University, Tianjin 300072*

[2] *Civil Aviation Meteorological Institute, Key Laboratory of Operation Programming & Safety Technology of Air Traffic Management, Civil Aviation University of China, Tianjin 300300*

(Received 8 March 2019)

As a crucial parameter for a few-cycle laser pulse, the carrier envelope phase (CEP) substantially determines the laser waveform. We propose a method to directly describe the CEP of an isolated attosecond pulse (IAP) by the vortex-shaped momentum pattern, which is generated from the tunneling ionization of a hydrogen atom by a pair of time-delayed, oppositely and circularly polarized IAP-IR pulses. Superior to the angular streaking method that characterizes the CEP in terms of only one streak, our method describes the CEP of an IAP by the features of multiple streaks in the vortex pattern. The proposed method may open the possibility of capturing sub-cycle extreme ultraviolet dynamics.

PACS: 32.80.−t, 33.20.−t, 42.25.Ja DOI: 10.1088/0256-307X/36/6/063201

The carrier envelope phase (CEP) of a few-cycle pulse determines the electric field, which correspondingly governs many strong field processes observed in attosecond physics.[1] Due to the availability of few-cycle CEP-stabilized laser pulses, the sub-cycle dynamics can be captured in atoms and molecules. In the past decades, many interesting phenomena have been studied employing CEP-locked few-cycle pulses. Kling *et al.*[2] explored the electron dynamic in a sub-cycle scale and steered the molecular breakup path. Lindner *et al.*[3] generated Young's double-slit-type interference in the photoelectron spectra by controlling the electron ejection at two possible instants. In 2001, Baltuška *et al.* produced supercontinuum high harmonics,[4] which could lead to an isolated attosecond pulse (IAP).[5] As a sophisticated technique for ultrafast sciences, the IAP opens the possibility of unprecedented high time resolution. By combining an attosecond extreme ultraviolet (EUV) pulse and an intense ultrashort IR pulse, a series of ultrafast processes, such as tunneling,[6] can be successfully observed.

The CEP characterization of a few-cycle strong IR pulse is mainly based upon tunneling ionization of atoms in the strong laser fields. Because the tunneling ionization is highly nonlinear, a slight difference of the laser waveform can be magnified in the photoelectron distribution. By observing it, the CEP information could be extracted in a single shot. Paulus *et al.*[7] proposed a CEP-measuring approach for few-cycle pulses on the basis of strong interaction between the laser and atoms. Wittmann *et al.*[8] applied the left-right asymmetries of photoelectrons emitted along the laser polarization to obtain the CEP information. Few-cycle IAPs have already been generated in many labs by different strategies.[9] Nevertheless, because the IAP thus obtained is too weak to keep a highly nonlinear state, the successful characterization of the CEP of a few-cycle IR pulse cannot be employed to describe the CEP of an IAP. Therefore, a few combination strategies[10] have been developed to generate energy or momentum spectra for IAP characterization. For instance, Liu *et al.*[10] presented an approach of two-color photoionization, where an attosecond waveform and a CEP-stabilized IR pulse were combined to generate coherent photoelectron spectra for extracting the CEP of an IAP. Amplifying the performance of the CEP of an IAP by coherent superposition is the essence of these approaches, in which a strictly stable CEP is the prerequisite. In addition, angular streaking was used for the CEP description of an IAP. The method employed an IR pulse and a superimposed circularly polarized IAP to ionize atoms, and described the CEP by photoionization momentum distributions. It opens the door to characterizing the CEP of a weak IAP accurately.

A few years ago, Ramsey interference[11] of laser-produced electron wavepackets was found to contain a totally new feature—vortex-shaped momentum spectra—when a pair of time-delayed and circularly polarized pulses were applied to ionize a molecule or atom. This novel discovery demonstrates that on the plane of the laser polarization,[12] the momentum distributions of ionized electrons will display vortex momentum spectra or spiral structure.[13] Only the counter-rotating circularly polarized pulses would generate vortex-shaped distributions, while the co-rotating ones just induce a Newton ring-like momentum distribution. Furthermore, this kind of vortex-shaped momentum spectrum has been verified experimentally in potassium atoms.[14] In addition, Li *et al.*[13] studied the photoelectron momentum patterns of helium ionized by bi-chromatic circularly polarized ultrafast laser pulses, and found that counter-

*Supported by the National Natural Science Foundation of China under Grant Nos 11674243 and 11674242

**Corresponding author. Email: johngzhang@tju.edu.cn

© 2019 Chinese Physical Society and IOP Publishing Ltd

rotating pulses could induce spiral momentum distribution. This is the first report on vortex-shaped momentum formation in a molecule. Then, Djiokap found vortex-shaped momentum distributions of zero-start, one-start, two-start, three-start and four-start for a UV carrier frequency of 15 eV and intensity of 1×10^{12} W/cm^2.[15]

Inspired by the pioneering investigation on the interference photoelectron spectra of hydrogen atoms and vortex momentum distributions of inert atoms, we propose a novel exciting-pulse combination that involves a pair of time-delayed IR pulses and a superimposed circularly polarized IAP. Deploying the strong field approximation (SFA) theory[16,17] in our numerical simulations, we investigate the characteristics of vortex-shaped momentum patterns in relation to the IAP CEP. Unlike the conventional angular streaking method that characterizes the CEP in terms of only one streak, our method describes the IAP CEP on the basis of the features of multiple streaks in the vortex-shaped momentum distribution, which increases the accuracy of the CEP characterization.

In our strategy, the IAP and the CEP-stabilized IR pulse are overlapped, and both are circularly polarized. The electric field relating to the pulses is polarized in the x–y plane of Cartesian coordinates. Its two components can be written as

$$\begin{aligned} E_x =& E_{0,\mathrm{IAP}}[\cos(\omega_{\mathrm{IAP}}t+\theta)+\cos(\omega_{\mathrm{IAP}}(t+T) \\ &+\theta)]\cos^2\left(\pi\frac{t}{\tau_{\mathrm{IAP}}}\right)+E_{0,\mathrm{IR}}[\cos(\omega_{\mathrm{IR}}t+\theta_{\mathrm{IR}})\hat{x} \\ &+\cos(\omega_{\mathrm{IR}}(t+T)+\theta_{\mathrm{IR}})]\cos^2\left(\pi\frac{t}{\tau_{\mathrm{IR}}}\right), \\ E_y =& E_{0,\mathrm{IAP}}[\sin(\omega_{\mathrm{IAP}}(t+T)+\theta)-\sin(\omega_{\mathrm{IAP}}(t) \\ &+\theta)]\cos^2\left(\pi\frac{t}{\tau_{\mathrm{IAP}}}\right)+E_{0,\mathrm{IR}}[\sin(\omega_{\mathrm{IR}}(t+T) \\ &+\theta_{\mathrm{IR}})-\sin(\omega_{\mathrm{IR}}t+\theta_{\mathrm{IR}})]\cos^2\left(\pi\frac{t}{\tau_{\mathrm{IR}}}\right), \end{aligned} \tag{1}$$

where the peak field amplitudes $E_{0,\mathrm{IR}}$ and $E_{0,\mathrm{IAP}}$ are calculated according to $E_0 = [I/(3.51\times10^{16})]^{1/2}$, θ and θ_{IR} indicate the CEPs of the IAP and IR pulse, respectively, T is the time delay between two pulses, and τ_{IR} and τ_{IAP} are the pulse durations of the IAP and IR pulse. Their carrier frequencies are named as ω_{IR} and ω_{IAP}.

The amplitude of the ionized electron reaching a final momentum p is expressed by the SFA formula[16]

$$\begin{aligned} f(\boldsymbol{p}) =& -i\int_{-\infty}^{\infty}dt'\exp(i\varphi)\Big\{\frac{2^{3.5}\times(2I_{\mathrm{p}})^{5/4}}{\pi} \\ &\cdot\frac{\boldsymbol{p}}{(\boldsymbol{p}^2+2I_{\mathrm{p}})^3}\Big\}\cdot\boldsymbol{E}, \end{aligned} \tag{2}$$

in which the so-called classical action phase can be written as

$$\varphi = \int_{t'}^{\infty}dt''\Big[I_{\mathrm{p}}+\frac{(\boldsymbol{p}+\boldsymbol{A})^2}{2}\Big], \tag{3}$$

where I_{p} is the ionization threshold of the hydrogen atom, and $\boldsymbol{A}$ indicates the vector potential of the field.

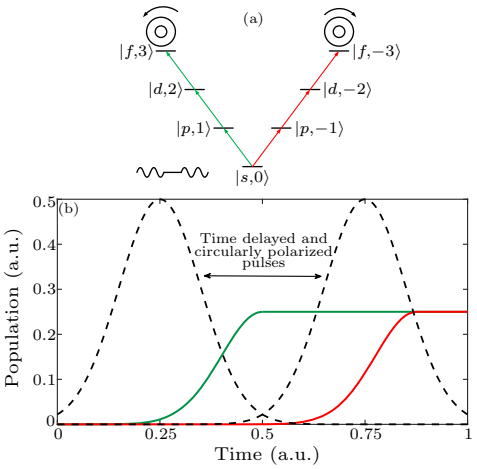

Fig. 1. Ionization scheme of hydrogen atoms with left- and right-handed circularly polarized pulses, involving the energy structure of the atom (a), as well as the coupling between the population of the atom and fields (b). The ionization pathways contain $|s,0\rangle \to |p,1\rangle \to \ldots \to |l,m\rangle$ (green), and $|s,0\rangle \to |p,-1\rangle \to \ldots \to |l,-m\rangle$ (red).

In our simulation, the wavelengths of the IR and IAP pulses are 800 nm and 67 nm, respectively. The maxima of the vortex-shaped momentum spectra can be described as Archimedean spirals. The energy separation of the vortex arms is determined by the intrapulse time delay. The pulse pairs beginning with a right-handed overlapped circularly polarized pulse and followed by a left-handed overlapped circularly polarized pulse (RLCP), can generate a counterclockwise-rotating electron vortex, whereas the clockwise-rotating electron vortices are created by pulse pairs with the reverse polarization ordering (LRCP). As shown in Fig. 2, a pair of IAPs are superimposed on the peak of two IR pulses, which can enhance the energy of the IAP for generating clear CEP-controlled momentum spectra. In our view, ionization with a left-handed circularly polarized pulse proceeds via the states of $|s,0\rangle \to |p,1\rangle \to \ldots \to |l,m\rangle$, followed by a right-handed one that proceeds via the states of $|s,0\rangle \to |p,-1\rangle \to \ldots \to |l,-m\rangle$. As shown in Fig. 1, the population of hydrogen atoms increases with the appearance of the time-delayed pulses via two ionization pathways, which leads to the coherent superposition state

$$|\psi\rangle \propto e^{-i\tau E/\hbar}|l,m\rangle + |l,-m\rangle. \tag{4}$$

According to the experiments and simulation,[18,19] if ω and T are within certain ranges, the magnetic quantum number m will satisfy

$$m \propto \frac{1}{\omega\cdot T}, \tag{5}$$

and determines the number of vortex arms directly in the photoionization momentum distribution. Because the superimposed pulses are the combination of time-delayed IAP and IR pulses, the two types of pulse are both responsible for the magnetic quantum number m. According to Eq. (5), m for the IR pulse is

undoubtedly much larger than for the IAP, thus the number of vortex arms is determined by the IR pulse pairs. On the other hand, the IAP also impacts the final photoionization momentum pattern significantly, which is mainly manifested as variations of the peak intensity, momentum, polar angle and torsion angle for different vortex arms. This phenomenon can be used for the IAP CEP characterization.

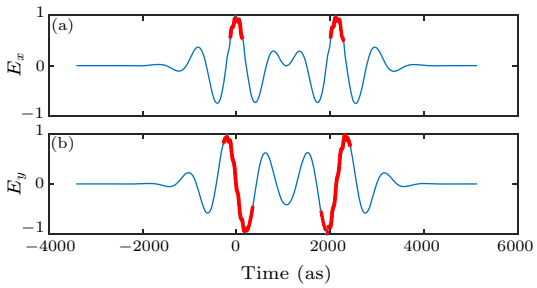

Fig. 2. Electric field patterns of the two time-delayed superimposed polarized attosecond pulses, projected on E_x (a) and E_y (b). The IAP CEP θ is $\pi/2$. The superimposed parts of the combined signals are highlighted in red.

To manifest the characteristics of the overlapped pulses, we show the electric field of the proposed pulse combination in the directions of E_x and E_x. In Fig. 2, it can be found that the electric fields along the two directions are different. For the E_x direction, the two time-delayed pulses are the same, while in the E_x direction, they are opposite. When $\theta \neq 0, \pi$, oppositely overlapped IAPs in the E_x direction will disturb the Ramsey interference of the combined IR-IAP pulses, which is associated with the IAP CEP. Therefore, by ionizing the atom with the proposed time-delayed superimposed pulses, we can obtain the vortex-shaped momentum distribution that carries the message of the IAP CEP.

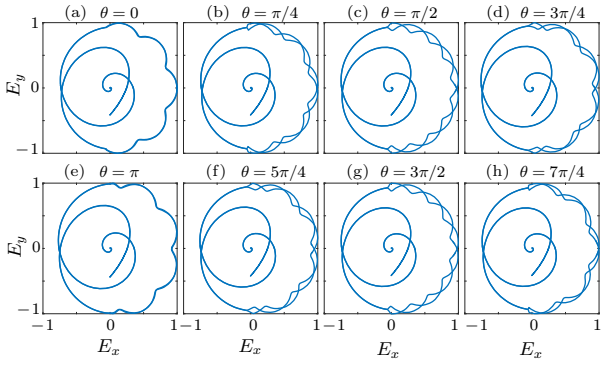

Fig. 3. Electric field patterns of two time-delayed superimposed polarized attosecond pulses. The parameters used in the simulation are: IAP CEP $\theta = 0$ (a), $\pi/4$ (b), $\pi/2$ (c), $3\pi/4$ (d), π (e), $5\pi/4$ (f), $3\pi/2$ (g), $7\pi/4$ (h), intensity $I = 3.5 \times 10^{14}\,\mathrm{W/cm^2}$, time delay $T = 2.5$ o.c., and pulse width $\tau = 2$ o.c.

In our view, the generation of the vortex-shaped momentum distribution is due to the Ramsey interference between photoelectron wave packets generated in the ionization of the atom by a pair of time-delayed, oppositely circularly polarized, IAP-IR overlapped pulses. Therefore, a slight change of the IAP CEP may seriously impact the characteristics of vortex arms in the momentum spectra. In Fig. 3, we plot the electric field patterns with varying IAP CEP θ of our proposed pulse combination in the E_x–E_y plane. For clarity, the parameters are set to be the following: time delay $T = 2.5$ optical cycle (o.c.) and intensity $I = 3.5 \times 10^{14}\,\mathrm{W/cm^2}$. It can be seen that the IAP of the superimposed pulses can significantly affect the distribution of the electric field. With the varying CEP of an IAP, $\theta = 0$, $\pi/4$, $\pi/2$, $3\pi/4$, π, $5\pi/4$, $3\pi/2$, $7\pi/4$, the overlapping position of two time-delayed pulses will change periodically in the plane of the electric field, which will result in the Ramsey interference of different IAP CEPs following a certain rule. When $\theta = 0$, the two time-delayed superimposed circularly polarized pulses are completely coincident in the electric field, thus the Ramsey interference of all the positions is even and strongest. Then, with the increase of the IAP CEP, the IAP parts of two coincident superimposed pulses start to separate from each other, as shown in Fig. 3(b). When the IAP CEP becomes $\pi/2$, the degree of separation of the two time-delayed IAPs reaches the maximum value, and correspondingly, the Ramsey interference of the two time-delayed IAPs shows its weakest value, which makes the Ramsey interference of all the positions uneven. Then, if the IAP CEP continues to increase, the IAP parts will begin to coincide, which boosts the Ramsey interference. Up to $\theta = \pi$, the IAP parts of two time-delayed pulses coincide, and the degree of Ramsey interference reaches the maximum value again. The Ramsey interference returns to an even state. Hereafter, the second similar period of the IAP CEP starts from $\theta = \pi$ to $\theta = 7\pi/4$, as exhibited in Figs. 3(e)–3(h). Due to the periodic feature of the IAP CEP, the electric field patterns in Figs. 3(b), 3(c) and 3(d) are similar to the those in Figs. 3(h), 3(g) and 3(f), respectively.

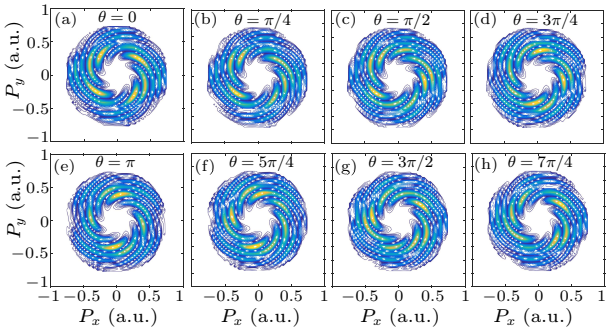

Fig. 4. The photoelectron momentum distribution in the polarization plane for ionization of hydrogen by the proposed time-delayed superimposed pulses. The parameters used in the simulation are: IAP CEP $\theta = 0$ (a), $\pi/4$ (b), $\pi/2$ (c), $3\pi/4$ (d), π (e), $5\pi/4$ (f), $3\pi/2$ (g), $7\pi/4$ (h), intensity $I = 3.5 \times 10^{14}\,\mathrm{W/cm^2}$, time delay $T = 2.5$ o.c., pulse width $\tau = 2$ o.c., and carrier frequency $\omega = 4$ eV.

Figure 4 exhibits the vortex-shaped momentum distribution for the proposed left- to right-handed superimposed pulse irradiating a hydrogen atom. It can be seen that when $\theta = 0$ and π, the vortex patterns are symmetric, otherwise, they are asymmetric, which is

due to the periodic change of the uniformity of Ramsey interference for the electric field. As shown in Figs. 4(a) and 4(e), two time-delayed circular pulses are completely coincident in the electric field when $\theta = 0$ and π, thus the corresponding degrees of Ramsey interference are strongest and even, which makes the vortex patterns symmetric. On the other hand, in Figs. 4(b)–4(d) and 4(f)–4(h), with the change of the IAP CEP, the Ramsey interference of the IAP becomes weaker, and the degrees of Ramsey interference of all the positions are uneven, which results in the asymmetric vortex arms. Moreover, because the change of the IAP CEP is periodic, the vortex-shaped momentum patterns of $\theta = \pi/4$, $\pi/2$ and $3\pi/4$ are centro-symmetric to the ones of $\theta = 7\pi/4$, $3\pi/2$ and $5\pi/4$, respectively. Obviously, these observations meet the characteristics of the electric field pattern for the combined pulses. Then we investigate the relationship between the IAP CEP and the symmetry states of the vortex-shaped momentum distribution, and find that the change of the IAP CEP is associated with the local rotation of the vortex arms. The variation of the IAP CEP can translate into the rotation of the electric field pattern and vortex arms, which maps into the change of the Ramsey interference degree. Therefore, the CEP of an IAP can be described by the characteristics of vortex arm rotation.

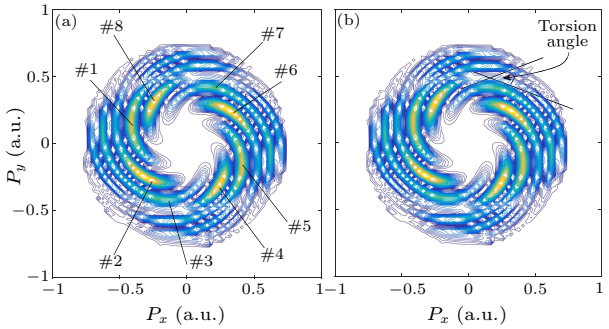

Fig. 5. In the photoionization momentum patterns, eight arms are named in (a), and the torsion angle is defined in (b).

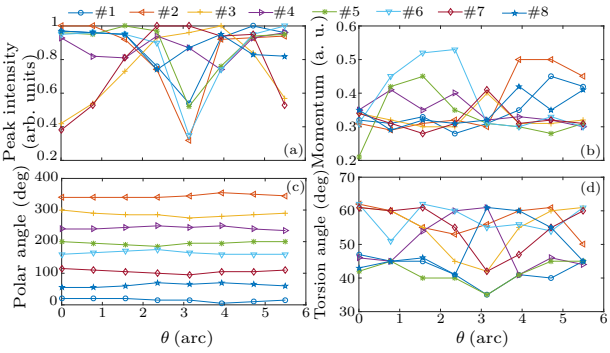

Fig. 6. Feature parameters of the vortex-shaped arms in the photoionization momentum distribution, plotted with respect to the IAP CEP: peak intensity (a), momentum (b), polar angle (c) and torsion angle (d).

Reviewing the above observations, the IAP CEP θ, as a significant parameter for a pair of time-delayed superimposed polarized pulses, is responsible for the overlapped electric field distribution that directly affects the characteristics of the vortex-shaped momentum pattern. To characterize the IAP CEP by the dynamic process of vortex momentum distribution in detail, we investigate the features of every vortex arm with varying θ. In Fig. 6(a), we exhibit the peak intensity of the vortex arm via the IAP CEP. It can be clearly observed that the peak intensities of the eight arms, as shown in Fig. 5(a), are symmetric about $\theta = \pi$, which meets the theory of periodic change of the IAP CEP. Similarly, in Figs. 6(b) and 6(d), the waveforms are still symmetric about $\theta = \pi$, which can be applied to simplify the process of the IAP CEP characterization. Additionally, one can also observe that the vortex arms can be divided approximately into two groups: 3 and 7, and the others. In the ranges of 0–$3\pi/4$ and $5\pi/4$–$7\pi/4$, the peak intensities of the 3 and 7 vortex arms are lower than those of the others, and have a nearly linear relationship with the IAP CEP, which is beneficial for the precise description of an IAP CEP. Nevertheless, in the range of $3\pi/4$–$5\pi/4$, the peak intensities of eight vortex arms are chaotic, which make the CEP characterization difficult. In Fig. 6(b), we demonstrate the relationship of the IAP CEP and vortex arm momentum in the photoionization momentum distributions. It can be found that the eight vortex arms can be classified into three groups. The momenta of the first group (2 and 6) are maximum, and have the highest rate of monotonous change with varying IAP CEP in the ranges of $\theta = 0$–$3\pi/4$ and $5\pi/4$–$7\pi/4$, which is also suitable for the CEP characterization. The momenta of the second group (5, 4, 7 and 8) are between those of the first group and the third group (1 and 3). Unlike the momenta of the first group, those of the second group are not monotonous. The third group (1 and 3) has the lowest momenta, which are almost unchanged by the IAP CEP.

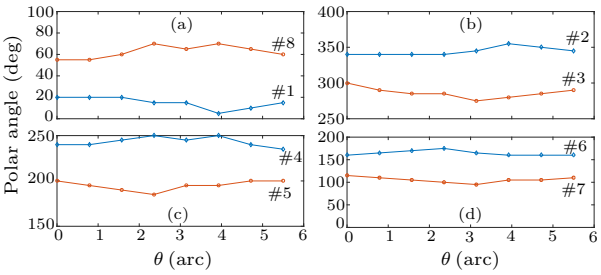

Fig. 7. The polar angles between the vortex arms (a) 1 and 8, (b) 2 and 3, (c) 4 and 5, and (d) 6 and 7 in the photoionization momentum pattern plotted with respect to the IAP CEP.

After focusing on the degree parameters of the vortex arms in the momentum distribution, we investigate the relationship between the angle parameters and the CEP of an IAP. In Fig. 6(c) the polar angles of the eight vortex arms are plotted versus the IAP CEP. For clarity, Fig. 6(c) is split into four figures shown in Fig. 7. Different from the so-called degree

parameters in Figs. 6(a) and 6(b), the angle parameters are very regular with varying IAP CEP. It can be seen that Figs. 7(a)–7(d) are reverse symmetric, respectively, and also meet the periodic theory of the IAP CEP. Moreover, in Figs. 7(b) and 7(d), the polar angles of the 3 and 7 vortex arms have good linear relationship with the IAP CEP in the ranges of π–$7\pi/4$ and 0–π, respectively. These relationship characteristics make the polar angle more beneficial for CEP characterization than degree parameters. In Fig. 6(d), we exhibit the relationship between the torsion angle (shown in Fig. 5(b)) and the IAP CEP. Unlike the polar angle in Fig. 6(c), the torsion angle via the IAP CEP demonstrates a complex relationship. It is difficult to classify the eight vortex arms by the torsion angle alone. However, one can find that the torsion angles of 3 and 7 have an approximately linear relationship with the IAP CEP in the ranges of 0–π and π–$7\pi/4$, which can also be used to describe the IAP CEP as an auxiliary method.

In summary, we have proposed a method based on the vortex-shaped momentum distribution to accurately characterize the IAP CEP. Based on the theories of electron vortices and Ramsey interference, we design a novel pulse combination that consists of two time-delayed, oppositely, circularly polarized, IAP-IR overlapped pulses. Ionizing the atom by them with varying IAP CEP, we can obtain a series of distorted vortex-shaped momentum patterns that vary with the IAP CEP following a certain rule. By deploying the SFA theory, we investigate the photoionization driven by the proposed combined pulses. We find that the size, position and orientation of the generated vortex arms are sensitive to the CEP of an IAP, and that these quantities of some specific vortex arms have a linear relationship with the IAP CEP, which can serve as an ideal method of characterizing the CEP of an IAP.

References

[1] Krausz F and Ivanov M 2009 *Rev. Mod. Phys.* **81** 163
[2] Kling M F, Siedschlag C, Verhoef A J, Khan J I, Schultze M, Uphues Th, Ni Y, Uiberacker M, Drescher M, Krausz F and Vrakking M J J 2006 *Science* **312** 246
[3] Lindner F, Schätzel M G, Walther H, Baltuska A, Goulielmakis E, Krausz F, Milosevic D B, Bauer D, Becker W and Paulus G G 2005 *Phys. Rev. Lett.* **95** 040401
[4] Hentschel M, Kienberger R, Spielmann C Reider G A, Milosevic N, Brabec T, Corkum P, Heinzmann U, Drescher M and Krausz F 2001 *Nature* **414** 509
[5] Baltuška A, Udem Th, Uiberacker M, Hentschel M, Goulielmakis E, Gohle Ch, Holzwarth R, Yakovlev V S, Scrinzi A, Hänsch T W and Krausz F 2003 *Nature* **421** 611
[6] Uiberacker M, Uphues Th, Schultze M, Verhoef A J, Yakovlev V, Kling M F, Rauschenberger J, Kabachnik N M, Schröder H, Lezius M, Kompa K L, Muller H G, Vrakking M J J, Hendel S, Kleineberg U, Heinzmann U, Drescher M and Krausz F 2007 *Nature* **446** 627
[7] Paulus G G, Lindner F, Walther H, Baltuska A, Goulielmakis E, Lezius M and Krausz F 2003 *Phys. Rev. Lett.* **91** 253004
[8] Wittmann T, Horvath B, Helml W, Schätzel M G, Gu X, Cavalieri A L, Paulus G G and Kienberger R 2009 *Nat. Phys.* **5** 357
[9] Sansone G, Benedetti E, Calegari F, Vozzi C, Avaldi L, Flammini R, Poletto L, Villoresi P, Altucci C, Velotta R, Stagira S, De Silvestri S and Nisoli M 2006 *Science* **314** 443
[10] Liu C D, Reduzzi M, Trabattoni A and Sunilkumar A 2013 *Phys. Rev. Lett.* **111** 123901
[11] Ramsey N F 1950 *Phys. Rev.* **78** 695
[12] Hasovic E, Becker W and Milosevi D B 2016 *Opt. Express* **24** 6413
[13] Yuan K, Chelkowski S and Bandrauk A D 2016 *Phys. Rev. A* **93** 053425
[14] Pengel D, Kerbstadt S, Johannmeyer D, Englert L, Bayer T and Wollenhaupt M 2017 *Phys. Rev. Lett.* **118** 053003
[15] Ngoko J M, Meremianin A V, Manakov N L, Hu S X, Madsen L B and Starace F 2017 *Phys. Rev. A* **96** 013405
[16] Klaiber M, Danek J, Yakaboylu E, Hatsagortsyan K Z and Keitel C H 2017 *Phys. Rev. A* **95** 023403
[17] Keldysh L V 1965 *Sov. Phys. JETP* **20** 1307
[18] Li M, Zhang G Z, Kong X L, Wang T Q, Ding X and Yao J Q 2018 *Opt. Express* **26** 878
[19] Li M, Zhang G Z, Ding X and Yao J Q 2018 *IEEE Photon. J.* **10** 3300109